*J. Fluid Mech.* (1981), *vol.* 105, *pp.* 327-345
*Printed in Great Britain*



# Turbulent convective velocities (broadband and wavenumber dependent) in a plane jet

By V. W. GOLDSCHMIDT, M. F. YOUNG AND E. S. OTT
Ray W. Herrick Laboratories, Purdue University School of Mechanical Engineering, West Lafayette, Indiana 47907, USA

(Received 23 July 1979 and in revised form 9 January 1980)

An investigation into the magnitude and direction of the convective velocity in a plane air jet was performed. Convective velocities were obtained from cross-correlation measurements. They are defined as the ratio of the spacing between two hot-wire probes and the time delay between their signals to reach maximum correlation. These velocities were larger in magnitude than the local mean velocities for lateral distances greater than the half-width of the jet. Frequency analysis of the convective velocity indicates that the large-scale eddies move slower than the mean flow while the small scales move faster. Based on the convective velocity vector, broadband 'convection lines' were defined and found to point outward with respect to the streamlines for all values of $y/b \geqslant 0{\cdot}5$. Likewise, frequency investigation indicates that 'convection lines' point outward for all $y/b \leqslant 1{\cdot}3$ and then inward for larger values of $y/b$.

## 1. Introduction

Space–time correlations, along with power spectra, are well established classical techniques for gaining information into the nature of turbulent flows. Correlations permit determination of the velocity by which the eddies are convected within the flow. This velocity of convection, or 'convective velocity', is often used to relate time to space scales of turbulence and to find the existing relationships between velocity and pressure fluctuations in the potential core and mixing regions of the jet.

In this work, the measure of space–time correlations, and hence convective velocity, has been obtained through normal time averages. The possibility of measures of conditional convective velocities, although an attractive alternative which may give further insight into the nature of the non-vortical flow 'driven' by the moving and engulfing interface, is not treated here. It is possible that weighted superposition of the turbulent and potential fields could explain some of the trends reported.

## 2. Convective velocity

Taylor's statistical approach suggests the use of two hot-wire anemometer sensors to determine the correlation of velocity fluctuations at different locations in the flow. Taylor's approximation (for a homogeneous flow) formally states that (Taylor 1935)

$$\partial/\partial t = -\overline{U}_1 \partial/\partial x, \tag{1}$$

where $\overline{U}_1$ is the local mean velocity.

0022-1120/81/4649-3300 $02.00 

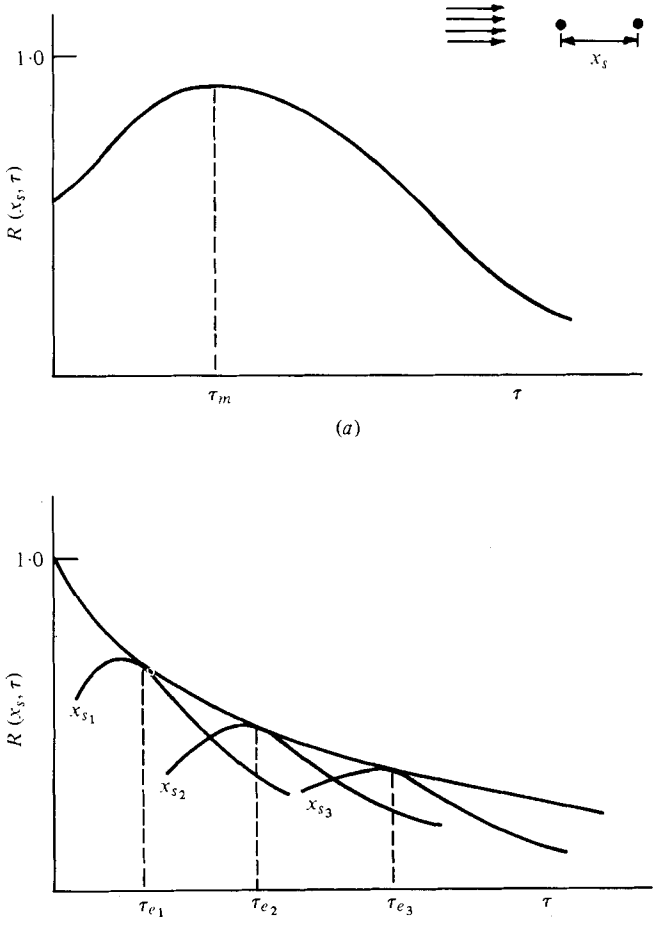


FIGURE 1. Space–time correlation curves. (*a*) The curve shows $R(x, \tau)$ for $x = x_s$. (*b*) Three curves show $R(x, \tau)$ for $x = x_{s_1}$, $x_{s_2}$ and $x_{s_3}$.

Lin (1953) showed that Taylor's hypothesis is invalid when large acceleration terms (caused by shear) are present. Sternberg (1967) used arguments based on vorticity to show that for shear flows in general (and boundary layers in particular) the disturbance (or convective) velocity at a point in the flow is usually different from the local mean velocity. Fisher & Davies (1964) investigated the frozen turbulence concept in the mixing region of an axisymmetric jet and found that the mean shear and high turbulent intensities create an uncertainty in the transformations between time and space dependence at a single point in the flow. They found the convective velocity to be frequency dependent, and as such not equal to the local mean velocity for all frequencies. This result casts doubts on the exact validity of Taylor's hypothesis in shear flow. However, numerous experiments have confirmed the applicability of Taylor's simplification for grid flows and in certain regions of wall shear flows.

There seem to be at least three different definitions of convective velocity in the literature (see appendix). The simplest definition is based on Taylor's hypothesis. If

a space–time correlation similar to that in figure 1 is measured, the convective velocity can then be defined as

$$U_c = x_s/\tau_m \,, \tag{2}$$

where $x_s$ is the separation between the probes and $\tau_m$ the time to reach maximum correlation. According to Taylor's hypothesis this value of $U_c$ should equal the value of the local mean velocity $U_1$. Thus, departure of the quantity $U_c/U_1$ from 1 gives an indication of the validity of Taylor's hypothesis. Experimenters using this definition for 'convective velocity' include Wygnanski & Fiedler (1969), Wilson & Damkevala (1970), Rotta (1962), Willmarth (1959), Oswald & Kibens (1971), and Favre, Gaviglio & Dumas (1967).

In the work now reported, the convective velocity $U_c$, as defined by (2), will be used. The objective is to determine the variation and direction of $U_c$ within the self-similar region of a plane jet as well as the applicability of Taylor's hypothesis. The reported work extends the results that are available in the literature and which have been summarized in the table in the appendix.

## 3. Experimental procedure and results

### 3.1. *Set-up*

The plane jet issued from a reactangular slit of width $D = 0{\cdot}635$ cm, and with an aspect ratio of 48. The exit Reynolds number was approximately $10^4$ based on an exit velocity $U_0$ of 23·77 m/sec. The usual checks for two-dimensionality (up to $X/D = 100$), momentum conservation and similarity were performed. The half-width was found to satisfy the relationship (for $10 \leqslant X/D \leqslant 70$)

$$\frac{b}{D} = 0{\cdot}0875\left(\frac{X}{D} + 8{\cdot}75\right), \tag{3}$$

whereas the axial velocity $U_m$ decayed as

$$\left(\frac{U_m}{U_0}\right)^{-2} = 0{\cdot}15\left(\frac{X}{D} + 1{\cdot}25\right) \tag{4}$$

(for $10 \leqslant X/D \leqslant 70$).

Two Disa 55F-11 probes were employed as detectors and Security Associates Anemometers as signal generators. The analysis of the signals (filtered and non-filtered) was made by a Saicor correlator (SAI-42). In determining the convective velocities the probes were kept at a zero angle of incidence ($\theta = 0$) with the mean flow and at the same $Z$ location. Probe separation $x_s$ was maintained at a constant value of 1·27 cm while traversing in the $x$ and $y$ directions. (A separation of 1·27 cm was chosen so as to minimize possible probe interference. Measurements taken with $x_s \geqslant 1{\cdot}27$ were found to be equivalent.)

### 3.2. *Broad-band analysis*

(*a*) *Magnitude*

The ratio of convective velocities to the local mean velocities were first obtained for broadband signal analysis (all frequency components). This is shown in figure 2. The ratio of the convective to local mean velocity is near unity for $y/b$ (dimensionless ratio

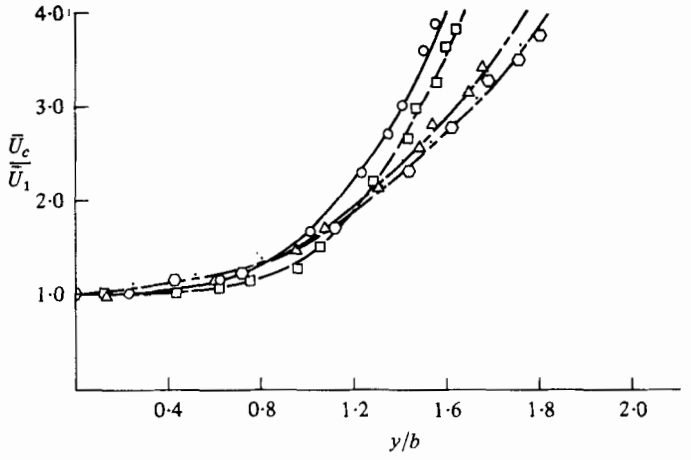


FIGURE 2. Convective velocities – broadband. ○, —, $x/D = 20$; □, — —, $x/D = 30$; △, ———, $x/D = 40$; ⬡, ···, $x/D = 60$.

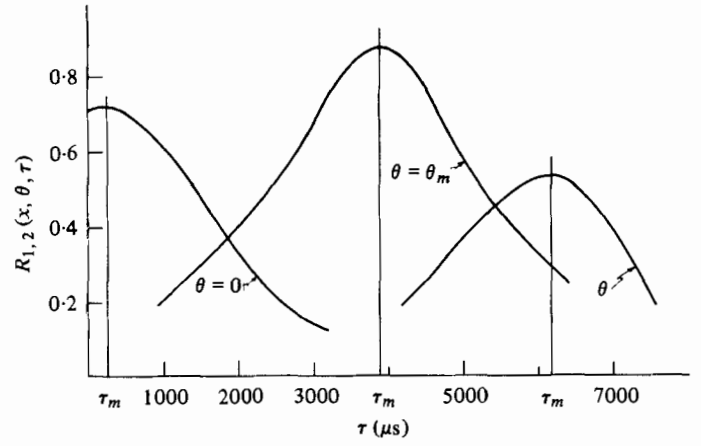


FIGURE 3. Correlation coefficient as a function of Θ. $x/D = 40$, $y/b = 0{\cdot}25$.

of lateral co-ordinate to half-width) less than 0·8 and increases for larger values of $y/b$. There is a dependence on $X/D$. For axial distances around 30 diameters the value of $U_c/U_1$ in the edges of the jet is larger than for locations around 60 diameters.

The noted values in the high-intermittency region of the jet are in agreement with Wygnanski & Fiedler (1969), Ott (1972) and others. The trends in the outer regions, for $y/b \geqslant 0{\cdot}8$, have been commented by Sternberg (1967), Wygnanski & Fiedler (1969), Ott (1972) and Favre *et al.* (1967).

(*b*) *Direction*

To determine the direction of the convective velocity, the probe system was rotated to different angles (measured in the $x$, $y$ plane) and the cross-correlation coefficient determined. Plots similar to figure 3 (for example) were generated. From these, the angle for maximum correlation and hence that defining the direction of the convective

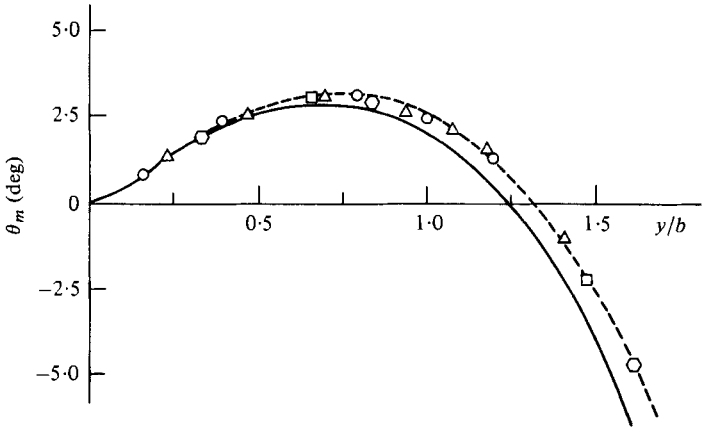


FIGURE 4. Angle of maximum correlation (broadband). ——, $\theta_v$; – – –, $\theta_m$. ○, $x/D = 20$; □, $x/D = 30$; △, $x/D = 40$; ⬡, $x/D = 60$.

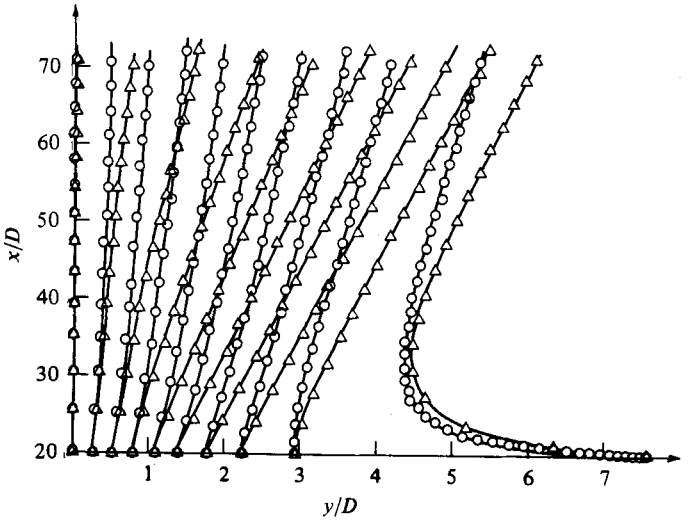


FIGURE 5. Streamlines and convection lines. ○, streamlines; △, convection lines.

velocity $\theta_m$ is obtained. Figure 4 shows $\theta_m$ *versus* lateral position $y/b$ for all $X/D$ stations (20, 30, 40 and 50) surveyed. Also shown in figure 4 is the direction of the mean velocity vector $\theta_v$ (determined from the classical solutions noted, for instance in Schlichting (1955)). For $y/b > 0{\cdot}4$ or so, $\theta_m$ becomes larger and is similar for all $X/D$ stations.

Figure 4, as it stands, does not relay as much information as would be obtained if 'convection lines' were plotted alongside streamlines. Convection lines may be defined as the trajectory of the turbulent structure determined by the corresponding convective velocity field. Computation of the streamlines was based on the measured $U$ and the $V$ obtained from mass conservation. The convection lines were determined postulating similarity and using the measured values of $u_c$ and $\theta_m$. Streamlines and convection lines, arbitrarily chosen so that they are coincident at $X/D = 20$, for

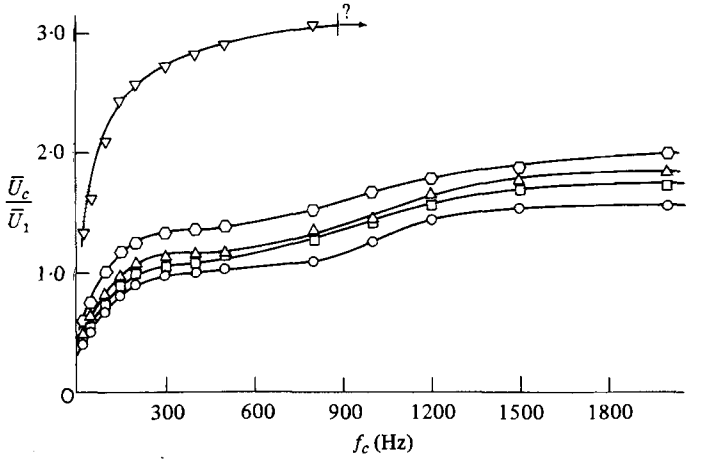


FIGURE 6. Convective velocity as a function of centre frequency $f_c$. $x/D = 20$. ○, $y/b = 0$; □, $y/b = 0{\cdot}5$; △, $y/b = 0{\cdot}75$; ⬡, $y/b = 1{\cdot}0$; ▽, $y/b = 1{\cdot}5$.

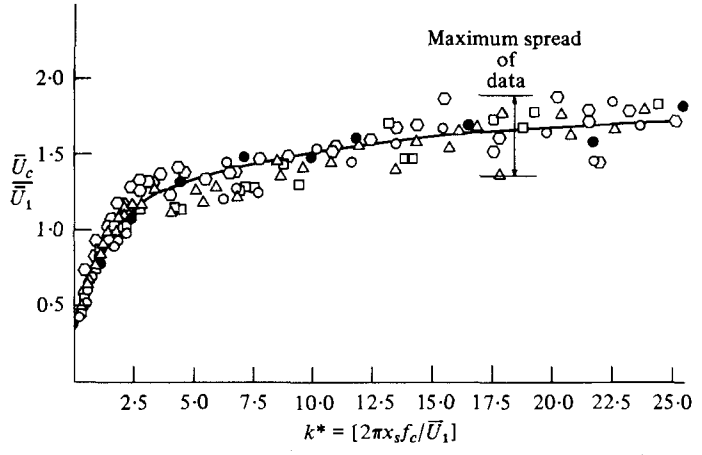


FIGURE 7. Convective velocities *vs.* dimensionless wavenumber. ○, $y/b = 0$; □, $y/b = 0{\cdot}50$; △, $y/b = 0{\cdot}75$; ⬡, $y/b = 1{\cdot}0$. Darkened circles represent data obtained for probe separation of 0·635 cm at $x/D = 40$ and $y/b = 0$.

example, and with a streamline spacing chosen to correspond to constant flow lines are shown on figure 5. The time interval between consecutive points along either set of lines is always of $10D/U_0$, as used in the computation scheme. It is interesting to note that in all cases the convection lines point further laterally than the streamlines and at the edges of the flow advance much more rapidly.

### 3.3. *Frequency-filtered analysis*

(*a*) *Magnitude.* A similar procedure to that employed for broadband investigation was used in the analysis of the convective velocity of different frequency components (filtered with Krohnite variable bandpass filters (model 310-C).

Centre frequencies investigated ranged from 25 to 2000 Hz. Measurements were

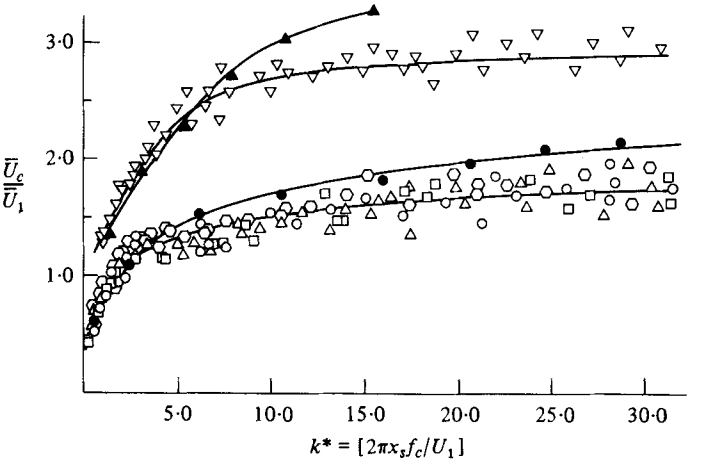


FIGURE 8. Convective velocity *vs.* dimensionless wavenumber. ○, $y/b = 0$; □, $y/b = 0{\cdot}5$; △, $y/b = 0{\cdot}75$; ⬡, $y/b = 1{\cdot}0$; ●, $y/b = 1{\cdot}25$; ▲, $y/b = 1{\cdot}5$; ▽, $y/b = 1{\cdot}75$.

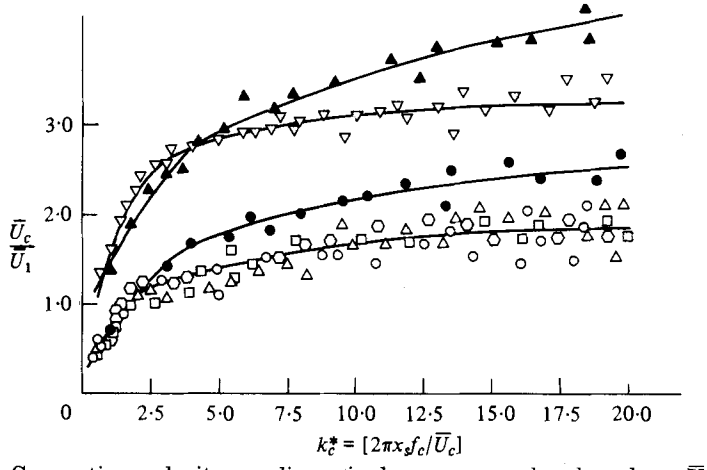


FIGURE 9. Convective velocity *vs.* dimensionless wavenumber based on $\bar{U}_c$. ○, $y/b = 0$; □, $y/b = 0{\cdot}5$; △, $y/b = 0{\cdot}75$; ⬡, $y/b = 1{\cdot}0$; ●, $y/b = 1{\cdot}25$; ▲, $y/b = 1{\cdot}50$; ▽, $y/b = 1{\cdot}75$.

taken at $X/D = 20$, 30, 40 and 60. As an example, figure 6 plots $U_c/U_1$ *versus* centre frequency $f_c$ for $X/D = 20$ at different $y/b$ locations. It indicates that the low frequencies (larger structures) move slower than the mean flow while the higher frequencies (smaller structures) move faster than the mean flow.

The results are best interpreted in terms of a dimensionless wavenumber (akin to a Strouhal number),

$$k^* = 2\pi x_s f_c/U_1, \tag{5}$$

where $x_s$ is the separation between probes, $f_c$ is the centre frequency, and $U_1$ is the local mean velocity. The measure of $U_c$ should be independent of the choices of $x_s$. The scaling length in (8) would best be the macroscale or some local length scale. $x_s$ is chosen strictly for convenience. It must also be noted that $k^*$ includes not only waves with a wavenumber $k$ aligned normal to $U_1$ but it also includes (due to aliasing) higher wavenumber components with a wave vector at an angle with $U_1$.

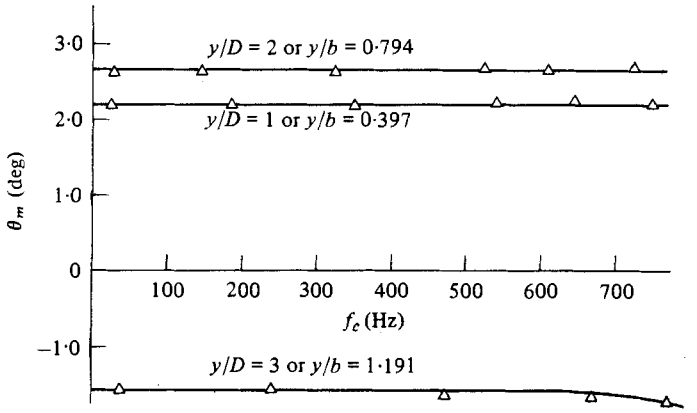


FIGURE 10. Angles for $\overline{U}_c$ as a function of frequency. $x/D = 20$.

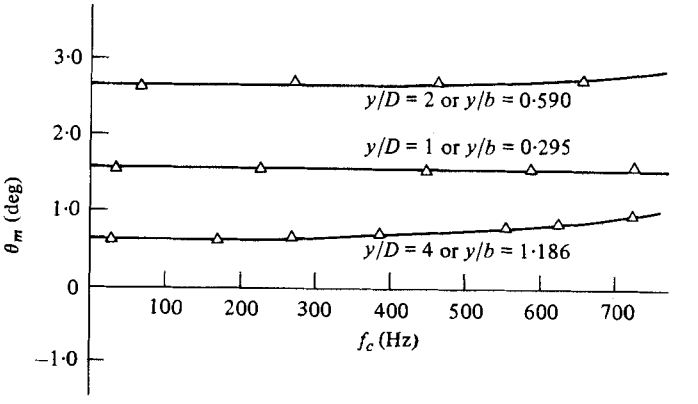


FIGURE 11. Angles for $\overline{U}_c$ as a function of frequency. $x/D = 30$.

A plot of $U_c/U_1$ *versus* $k^*$ number is shown in figure 7. All $X/D$ stations are represented, but the dimensionless lateral co-ordinate $y/b$ is limited to values less than or equal to unity. Similarity is evident and confirms data obtained by Favre (1965), Favre *et al.* (1967), Fisher & Davies (1964) and Wooldridge, Wooten & Amaro (1972) that the lower wavenumbers (large-scale disturbances) move slower than the higher wavenumber (small-scale) structures. If the data for $y/b > 1{\cdot}0$ is included (figure 8), a single curve does not result, although the trend is consistent.

The dimensionless wavenumber of figures 7 and 8 was based on the local mean velocity. It could be argued that it should be based on the convective velocity instead, or

$$k_c^* = 2\pi x_s f_c / U_c. \tag{6}$$

The ratio of the velocities $U_c/U_1$ is plotted against $k_c^*$ in figure 9. The results still show considerable differences along different lateral locations in the intermittent region of the flow. This may be partly attributed to the varying scales in the lateral direction and maybe to the intermittent nature of the flow as well.

(*b*) *Direction.* To obtain the angle of maximum correlation $\theta_m$ at each centre frequency, the same procedure was followed as that in determining $\theta_m$ for the broad-

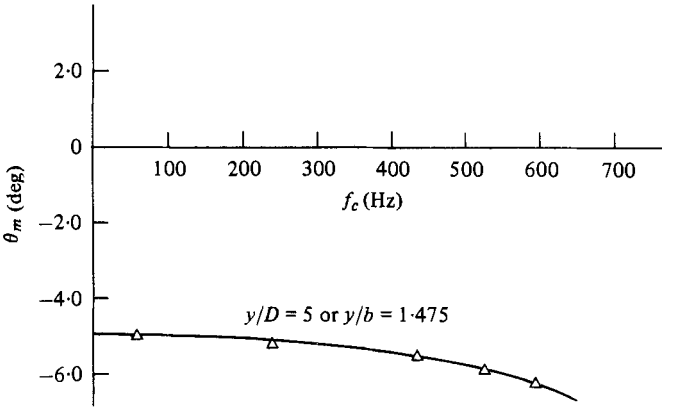


FIGURE 12. Angles for $\bar{U}_c$ as a function of frequency. $x/D = 30$.

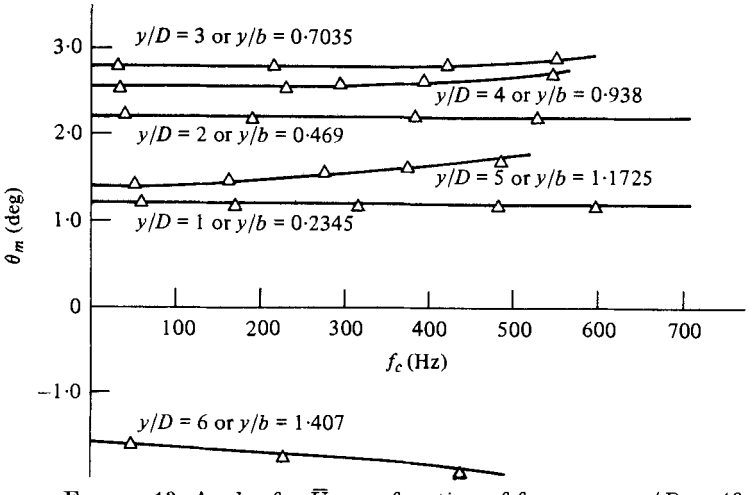


FIGURE 13. Angles for $\bar{U}_c$ as a function of frequency. $x/D = 40$.

band. The dependence of $\theta_m$ on $f_c$ at various $X/D, y/b$ stations is shown in figures 10–14. (The signal-to-noise ratio for centre frequencies in the order of 800 and larger becomes too small primarily in the edges of the jet.) Two observations are in order. First, in general for $y/b \leqslant 1{\cdot}3$, the angle $\theta_m$ is positive and increases with frequency. This means that, in the usual time-average perspective, the small scales move outwards farther as well as faster. On the other hand, for $y/b > 1{\cdot}3$, $\theta_m$ is negative with slightly larger negative values for increasing frequency. This means that the smaller scales appear to move inwards faster and farther. Secondly, comparing the broadband angles of figure 5 with the values of $\theta_m$ for the largest eddies (i.e. the intercepts of the ordinate, of figures 10–14, see figure 15), it is seen that the larger scales move closer to the mean velocity.

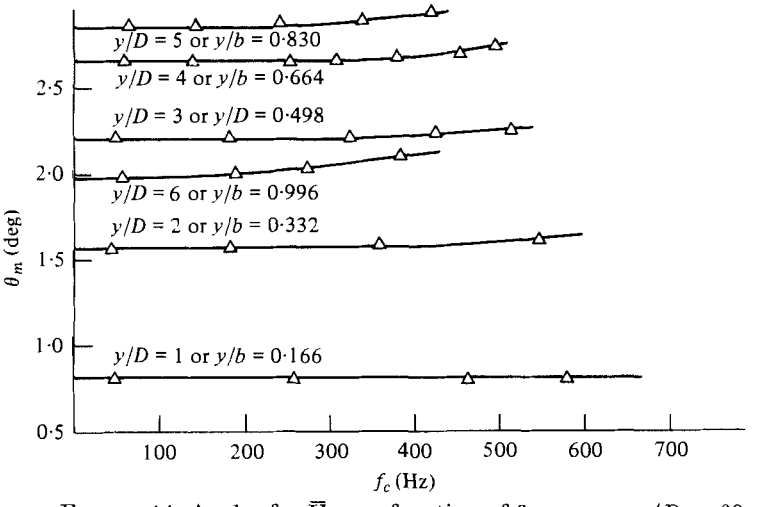


FIGURE 14. Angles for $\overline{U}_c$ as a function of frequency. $x/D = 60$.

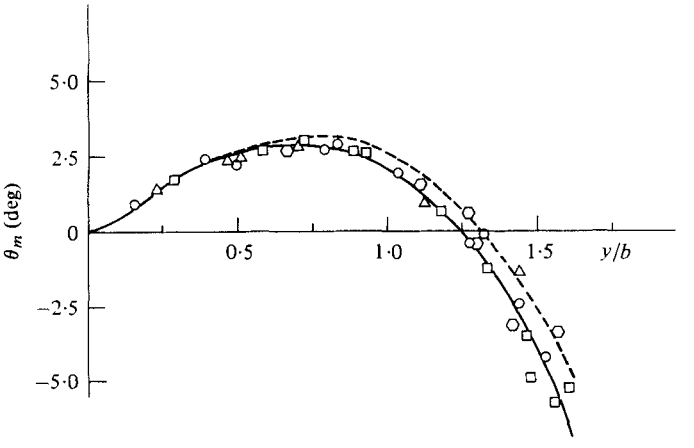


FIGURE 15. Angle of maximum correlation, both frequency and broadband. ——, $\theta_v$; – – –, $\theta_m$ at $f_c = 0$. ○, $x/D = 20$; □, $x/D = 30$; △, $x/D = 40$; ⬡, $x/D = 60$

## 4. Discussion and conclusions

The broadband measurements presented indicate that the ratio of the convective velocity to the local mean velocity is greater than unity for $y/b > 0{\cdot}8$. In the 'self-similar' region of the jet Taylor's hypothesis is valid for $y/b \leqslant 0{\cdot}8$. This corresponds to convective velocities nearly equal to the local mean velocities. For $y/b$ positions greater than 0·8 the convective velocity was noted to decrease slower than the local mean velocity.

Frequency analysis indicated that the large-scale motions move slower than the local mean flow while the small scales move faster. Broadband 'convection lines' lead the streamlines for $y/b \geqslant 0{\cdot}5$. They follow the streamlines for values $y/b < 0{\cdot}5$. For frequency analysis the 'convection lines' follow the streamlines at low frequencies

| $\eta$ $(y/b)$ | Convective velocity $U_c/U_1$ | From Robins's data $1+\overline{uu_i^2}/U_1\overline{u_i^2}$ |
|---|---|---|
| 0 | 1·0 | 1·0 |
| 0·5 | 1·17 | 1·04 |
| 1·0 | 1·56 | 1·20 |
| 1·5 | 2·47 | 1·64 |
| 2·0 | ~5·4 | 2·64 |

TABLE 1. Comparison of bulk velocity and convective velocity.

(large scales). Small scales first point outwards further than the streamlines, where for $y/b > 1{\cdot}3$ they reverse in trend, pointing inwards more than the larger scales.

The trends noted, essentially a convective pattern in which the larger-scale structures move slower than the smaller scales, is in agreement with the results of Heidrick, Banerjee & Azad (1977) for a pipe flow, Rajagopolan & Antonia (1979) in channel flows, Batt (1977) and Jones, Planchon & Hammersley (1973) for mixing layers, and Wygnanski & Fiedler (1969) and Wooldridge *et al.* (1972) in axial jets. They do disagree with part of the data in Heidrick, Azad & Banerjee (1971) near the wall of pipe flow and Dinkelacker *et al.* (1977) for pressure patterns beneath a boundary layer. McConachie, Bullock & Kronauer (1977) also find a higher convection velocity for the smaller wavenumbers (at a given filter centre frequency).† A word of caution is, however, in order. McConachie *et al.* are probably the only ones having a true wavenumber dependence defined. They obtained this through a transformation from spatial co-ordinates to wavenumber space. In all the other cases reported with a selective filtering (this work included), an unavoidable aliasing is taking place. The frequency-filtered signals include higher-wavenumber components not aligned along $U_1$. It is possible, however, that the presence of the wall and nature of the shear could also be having an effect on the preferential motion of the different-sized structures clearly underscoring the dangers in the common temptation to generalize from one type of flow to another.

A second common temptation is to relate the nature of instabilities to the structure of fully developed turbulence. Data on propagation of instabilities, such as that attributed to disturbances in the free shear layer, have been noted to exhibit a decreasing velocity of propagation with increasing frequency of the disturbance (for instance, see Bechert & Pfizenmaier 1975, Miksad 1972 and Hussain & Zaman 1978). This is also contrary to the results now reported supposedly in a fully developed turbulent flow. The differing distribution of convective (or phase) velocity with frequency (or wavenumber) of the structure of the disturbance under the above alternative conditions should be serious enough caution against this comparison.

A bulk convection velocity is used by Bradshaw, Ferriss & Atwell (1967) for boundary-layer calculations and similarly by Robins (1973) in a plane jet. Using Robins data such a velocity may be approximated by

$$U+\overline{uu_i^2}/\overline{u_i^2}, \tag{7}$$

giving the results of table 1 (for sufficiently large $X/D$ stations).

† On the other hand, in a non-sheared grid flow, Sepri (1976) finds no change of the convection velocity with wavenumber.

| | | $\Lambda_x/\Lambda_x$ (at $y = 0$) | |
|---|---|---|---|
| $X/D$ | $y/b$ | Based on $U_1$ | Based on $U_c$ |
| 20 | 0·086 | 1·02 | 1·02 |
| | 0·516 | 0·99 | 1·50 |
| | 0·945 | 0·85 | 1·31 |
| | 1·375 | 0·68 | 1·90 |
| | 1·81 | 0·28 | 1·41 |
| 30 | 0·058 | 0·99 | 0·99 |
| | 0·647 | 1·35 | 1·49 |
| | 0·941 | 1·03 | 1·38 |
| | 1·235 | 0·86 | 1·73 |
| | 1·53 | 0·66 | 2·13 |
| 40 | 0·044 | 0·99 | 0·99 |
| | 0·489 | 1·27 | 1·38 |
| | 0·934 | 0·91 | 1·32 |
| | 1·154 | 0·65 | 1·23 |
| | 1·378 | 0·52 | 1·22 |
| 60 | 0·10 | 1·01 | 1·01 |
| | 0·383 | 1·19 | 1·24 |
| | 0·972 | 1·09 | 1·67 |
| | 1·59 | 0·50 | 1·36 |

TABLE 2. Distribution of macroscales (determined from energy spectrum).

The difference between the above values may be in part attributed to the pressure–velocity correlation term ignored in the bulk velocity approximation of Robins (1973). On the other hand it is quite possible that the different values are attributed to different scales or wavenumber distributions governing the correlations and the energy transport.

The Taylor micro- and macroscales $\lambda, \Lambda$ are sometimes used to characterize turbulent flows. They are usually determined from the integral and parabolic approximations to the spatial correlations. Alternatively, they are sometimes approximated from the intercept and the integral of the second moment of the energy spectrum together with a descriptive mean velocity. The proper velocity to use is the convective velocity as it more closely relates the time and spatial turbulent scales although in its absence the local mean velocity is used instead. Accounting for the proper convective velocity the longitudinal microscales are seen to increase with lateral distance from the axis (this was reported in Goldschmidt & Young (1975)) contrary to the otherwise inferred constancy of $\lambda$ along $y/b$ or decrease along $y/b$ – as in Gutmark & Wygnanski (1976).

The longitudinal macroscales along the axis increase linearly with distance from a virtual origin and with a slope comparable to that of the velocity half width, as expected based on similarity concepts. The lateral distribution of the macroscales determined from the autocorrelation or the energy spectrum will depend on whether $U_1$ or $U_c$ is used in this estimate. Typical values computed are noted in table 2.

The trend inferred by not accounting for the convective velocity differing from the local mean velocity is that of a longitudinal integral scale decreasing in size with lateral location. On the other hand, properly considering the convective velocities measured shows a much more acceptable description: the sizes of the large structures

gradually increase with lateral location, at least up to a point near that where the interface has the highest probability of occurrence (i.e. $y/b = 1{\cdot}6$ as in Jenkins & Goldschmidt (1976)). Thereafter a slight tendency for a decrease in scale might be present. Although the present data is not sufficient to confirm it, this is in agreement with the data of Gutmark & Wygnanski (1976) based on two-point velocity-correlation measurements. This further exhibits the need for proper accounting of convective velocities when interpreting some of the statistical properties of turbulent flows. (See also Antonia, Phan-Thien & Chambers 1979.)

The work now reported was partially sponsored by the NSF and the ONR. Final phases of the work were completed while the first author was hosted (as a Fulbright Senior Scholar) by the Department of Mechanical Engineering at the University of Queensland. Their support, and that of the Australian American Educational Foundation are gratefully acknowledged.

## Appendix. Alternative definition of convection velocity

The definition of convection velocity used in this work was given in (2).

An alternative definition was made by Fisher & Davies (1964). It is based on a series of cross-correlation curves at different probe separations (measured along the direction of the mean flow) as shown in figure 1*b*. An envelope drawn tangent to these curves is then an auto-correlation function of the turbulent structure moving with a frame of reference in which the change of the turbulent structure is minimized. This suggests the definition of a convective velocity as the ratio of the probe separation $x_s$ to the time delay $\tau_e$, for which the correlation envelope is tangent to the space–time correlation curve for the separation, or

$$U_{c_1} = x_s/\tau_e. \tag{A 1}$$

This definition has been used by Davies, Fisher & Barratt (1963), Willmarth & Wooldridge (1962), Wooten *et al.* (1971), Bradshaw *et al.* (1964), Wygnanski & Fiedler (1969), Favre *et al.* (1967), Champagne, Harris & Corrsin (1970), Wills (1964), Ko & Davies (1971), and Bull (1967) among others.

The distinction between $U_c$ and $U_{c_1}$ has been discussed by Wills (1964), Favre *et al.* (1967), Comte-Bellot & Corrsin (1971), Wygnanski & Fiedler (1969), and Champagne *et al.* (1970).

Consider a typical plot of constant or iso-correlation curves versus time delay and probe separation as in figure 16. According to Fisher & Davis (1964), $U_{c_1}$ is equal to the ratio $x_m/\tau_e$ for $\partial R(x,\tau)/\partial x = 0$ as defined by Wills (1964). Fisher & Davis (1964) point out that Wills' definition and their own are equivalent except that theirs is easier to determine experimentally.

Further consideration of figure 16 reveals that a third definition for $U_c$ may be suggested as the ratio $x/\tau$ for which $\partial R(x,\tau)/\partial x = -\partial R(x,\tau)/\partial \tau$. This better approximates Taylor's hypothesis, in which there is a direct relationship between space and time. Such a definition $U_{c_2}$ would simply be the tangent of the angle with which the iso-correlation curves are skewed with respect to the time axis. Davis *et al.* (1963) use this definition in presenting their data although they make mention of the definition of $U_{c_1}$ suggested by Fisher & Davies (1964). Interestingly, in a footnote the latter authors suggest that $U_c$ is the velocity of the frame of reference where the spatial and temporal

| Reference (first author) | Flow field and region | Region of test | Definition of $U_c$ | $U_c/U_0$ |
|---|---|---|---|---|
| Bradshaw[1] | Round jet noise production region | $X/D = 2$<br>$0{\cdot}6 < y/b < 1{\cdot}5$ | $U_{c_1}$ | 0·8–0·1 |
| Bruun (1977) | Round jet | $X/D = 2$<br>$-0{\cdot}1 < y/x < 0$ | $U_c$ | 0·6–0·68 |
| Davies[1] (1963) | Round jet potential core mix region | $X/D = 1{\cdot}5, 4{\cdot}5$<br>$-0{\cdot}1 < (y-\frac{1}{2}D)/X < 0{\cdot}2$ | $U_{c_2}$ | 0·61–0·2 |
| Law (1975) | Round jet | Within $X/D < 3$ | $U_c$ | 0·63–0·69 |
| Davis[2] (1975) | Round jet supersonic | $9 < X/D < 25$<br>$0 < Y/X < 0{\cdot}1$ | $U_c$ | 0·7–0·4 |
| Wills[1] (1964) | Round jet<br>$D = 2$ in. | $X/D = 2$<br>$0{\cdot}3 < y/b < 0{\cdot}8$ | $U_{c_1}$ | 0·8–0·1 |
| Wilson[2] (1970) | Round jet<br>$D = 1$ in. | $X/D = 3$<br>$-0{\cdot}1 < (y-\frac{1}{2}D)/x < 0{\cdot}6$ | $U_c$ | 0·667 |
| Wygnanski[3] (1969) | Round jet<br>$D = 1{\cdot}04$ in. | $30 < X/D < 75$<br>$0 \leqslant y/x \leqslant 0{\cdot}15$ | $U_c$<br>$U_c$ | $U_{c_1}$ 1·05–0·4<br>$U_{c_2}$ 0·9–0·3 |
| Favre[4] (1967) | Boundary layer | 0·7<br>$y/\delta = \{0{\cdot}25\}$<br>0·03 | $U_c$<br><br>$U_{c_1}$ | 0·86<br>0·97<br>1·0–1·28 |
| Favre[5] (1967) | Boundary layer | $y/\delta = 0{\cdot}24$ | $U_c$ | 0·8 |
| Kovasznay[6] | Boundary layer | $y/\delta = 0{\cdot}6$ | $U_c$ | 0·93 |
| Favre[7] (1965) | Grid<br>$M = 1$ in. | $X/M = 40$ | $U_c$ | 1·0 |
| Comte-Bellot[7] (1971) | Grid<br>$M = 5{\cdot}08$ cm | — | $U_c$ | 1·0 |
| Champagne[8] (1970) | Homogeneous shear flow | — | $U_c$<br>$U_{c_1}$ | $\sim 1{\cdot}0$<br>$\sim 1{\cdot}0$ |
| Sepri (1976) | Heated grid | — | $U_c$ | $\geqslant 1{\cdot}0$ |
| Frenkiel (1966) | Grid<br>$M = 2{\cdot}54$ cm | — | $U_c$ | 1·0 |
| Demetriades (1976) | Supersonic wake flow | — | $U_c$ | $\sim 1{\cdot}0$ |
| Oswald[9] (1971) | Wake of disk | — | $U_c$ | 0·99 |
| Baldwin[7] (1961) | Pipe<br>$D = 8$ in | Centre-line | $U_c$ | 1·16 |
| Heidrick (1971) | Pipe<br>$D = 3{\cdot}1$ in. | Near wall centre-line | Lumley's | $> 1$<br>$\leqslant 1$ |
| Wygnanski (1970) | Two-dimensional mixing region | — | $U_{c_1}$ | 0·85 |
| Batt (1977) | Two-dimensional mixing region | — | $U_c$ | $< 1$ |
| Wooldridge (1972) | Round jet core and mixing region<br>$D = 1{\cdot}5$ in. | $X/D = 2$<br>$y/b = 0{\cdot}4$ | $U_{c_1}$ | 0·68 |
| Chanaud[7] (1970) | Wall jet | — | $U_c$ | 0·5 |
| Ko (1971) | Round jet<br>$D = 2{\cdot}5$ cm | $X/D = 1{\cdot}5$<br>$y/b =$ core | $U_c$ | 0·65–0·75 |

| Reference (first author) | Flow field and region | Region of test | Definition of $U_c$ | $U_c/U_0$ |
|---|---|---|---|---|
| Bull[10] (1967) | Boundary layer | — | $U_{c_1}$ | 0·53–0·825 |
| Willmarth[10] (1962) | Boundary layer | $y/\delta = 0$ | $U_{c_1}$ | 0·56–0·83 |
| Blackwelder (1977) | Boundary layer | $y^+ = 15$ | — | 0·8 |
| Willmarth (1959) | Pipe $D = 4$ in. | $y/\delta = 0$ | $U_c$ | 0·82 |
| Crocos[11] | Pipe | $y/\delta = 0$ | $U_c$ | 0·9–0·8 |
| McConachie[12] (1977) | Pipe | $Y^+ = 70$ | $U_c$ | — |
| Rajagopalan[13] (1980) | Channel | $0 < y/D < 1$<br>$y/D = 0$ | $U_c$<br>$U_c$ | 0·68–0·96<br>0·62 |
| Antonia (1979) | Atmospheric | $Z = 12$ metres | $U_c$ | 0·58–0·89 |

[1] Plots of $U_c vs. y/b$ and $U_c/U_m vs. y/b$ for Wills, Davies, Bradshaw, and Ko are nearly identical in the core and mixing region.

[2] Used cross-schlieren system. Wilson found $U_c$ constant across $y$ in the core and mixing regions, Davis went further on $X/D$ and found $U_c$ always less than $U$ (except for one traverse at $X/D = 9$).

[3] Measured $U_c/U_m vs. y/b$ for varying $X/D$, and found $U_c$ varies more slowly than $U_m$ across the jet.

[4] Found $U_c$ and $U_{c_1}$ a function of $y/\delta$.

[5] Data is reported by Rotta (1962).

[6] $U_c$ went from 0·92 to 0·97 for $y/\delta$ increasing from 0·6 to 1·2.

[7] The author's calculation.

[8] $U_c$ and $U_{c_1}$ differ by 2%.

[9] $U_c$ is nearly constant across the wake.

[10] $U_{c_1}$ increases with probe separation.

[11] Data is reported by Favre (1965). $U_c$ decreases with frequency.

[12] Measured as correlations in narrow frequency bands. Lower frequencies measured have values of $U_c$ around 12% higher than local mean velocity whereas for highest frequencies the convective velocity is around 75% of the local mean.

[13] Away from $y/D = 0$ based on velocity correlations; at $y/D = 0$ based on shear stress fluctuations.

TABLE 3. Convection velocity based on velocity signals.

rates of change of the pattern are of equal magnitude but opposite in sign; however, the plot in figure 16 shows that this is $U_{c_2}$ instead of $U_c$.

We can now distinguish three convective velocities: $U_c$, which minimizes the change of the maximum correlation with respect to time only, $U_{c_1}$ which minimizes the decay of maximum correlation in both time and space; and $U_{c_2}$ in which the rates of change of correlation in space and time are equal. All of these definitions coincide in a truly frozen field of turbulence.

Quantitatively the above are not very different. For nearly homogeneous turbulence, Champagne *et al.* (1970) show that $U_c$ is about 2% greater than $U_{c_1}$ as would be expected in the nearly frozen field. Wygnanski & Fiedler (1969) found $U_c$ to be from 10 to 20% greater than $U_{c_1}$ depending on the location in a round jet.

Comte-Bellot & Corrsin (1971) made an interesting analysis of the difference between

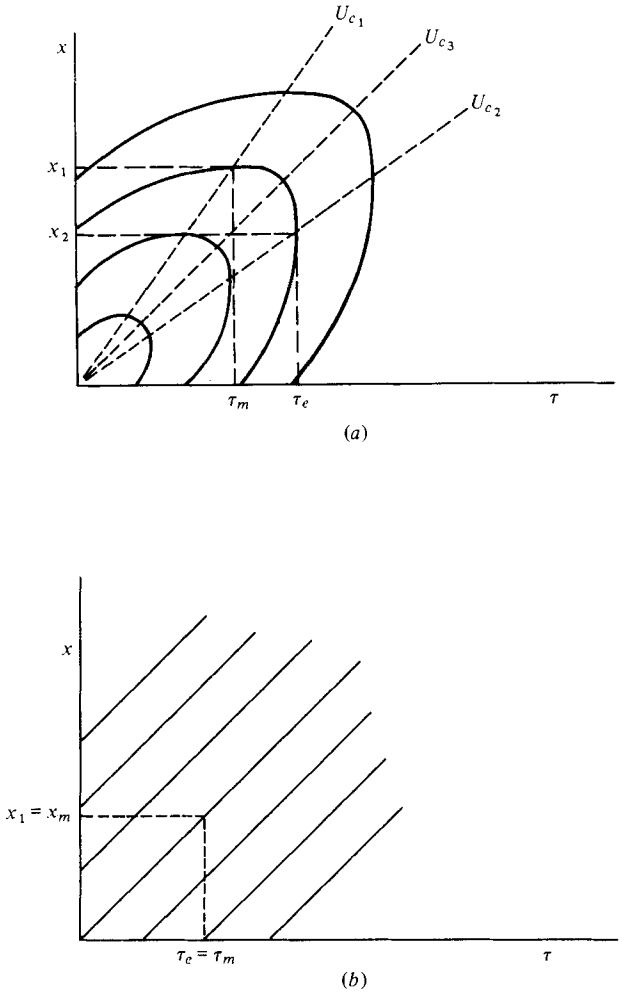


FIGURE 16. Iso-correlation curves, i.e. constant $R$.

the time delay $\tau_m$ to the peak in the space–time correlation curve, and the time delay $\tau_e$ to the tangent point on this curve to the moving axis auto-correlation that defines $U_{c_1}$. They suggest for a homogeneous isotropic field that $\tau_m$ will be related to $\tau_e$ by the expression

$$\tau_m = \tau_e/(1+u'^2/U_1^2). \tag{A 2}$$

From (2) and (3), then

$$U_c/U_{c_1} = (1+u'^2/U_1^2), \tag{A 3}$$

comparable to the more general expression in Heskestad (1965). For an example, in Champagne *et al.* (1970) where the turbulent intensity for grid flow is 0·019, $U_c/U_{c_1}$ was reported to be 1·02. Wygnanski & Fiedler's data reveal a turbulent intensity, $U'^2/U_1^2$, between 8 and 20 %. If Comte-Bellot & Corrsin's analysis for isotropic turbulence is extended to the jet shear flow, a value slightly larger than 1·08–1·20 would be expected for $U_c/U_{c_1}$. Wygnanski & Fiedler report values between 1·10 and 1·20. Thus, at least for turbulent intensity less than or equal to 20 % this analysis can be used to give a good estimate of $U_{c_1}$ from $U_{c_1}$ which is by far the easier to determine experimentally.

Experimental work in shear flows has demonstrated that different frequency components of the turbulent flow are convected with different velocities (and not necessarily equal to the mean velocity). Wills (1964) notes that in such flows the usual definitions of $U_c$ ($U_c$ and $U_{c_1}$) may lead to ambiguous results. Wills (1964), Lumley (1965), and Heidrick *et al.* (1971), among others, have suggested more refined definitions for $U_c$ to take its likely frequency dependence into account.

A fourth definition for $U_c$ was put forth by Favre *et al.* (1967). They define a convective velocity (noting symmetry with respect to space and time of the iso-correlation plots)

$$U_{c_3} = (U_c U_{c_1})^{\frac{1}{2}}. \tag{A 4}$$

For all practical purposes, $U_{c_3}$ is closer to $U_{c_2}$ than $U_c$ or $U_{c_1}$. Results available in the literature, indicating the definitions employed, are noted on table 3.

## REFERENCES


ANTONIA, R. A., CHAMBERS, A. J., FRICKE, G. A. & VAN ATTA, C. W. 1979 Temperature ramps in the atmospheric surface layer. *J. Atmos. Sci.* **36**, 99–108.

ANTONIA, R. A., PHAN-THIEN, N. & CHAMBERS, A. J. 1979 Taylor's hypothesis and the probability density functions of temporal velocity and temperature derivatives in a turbulent flow. *Univ. of Newcastle*, TN FN 34, Newcastle, Australia.

BALDWIN, L. V. & WALSH, T. J. 1961 Turbulent diffusion in the core of fully developed pipe flow. *A.I.Ch.E. Journal*, **7**, 30.

BATT, R. G. 1977 Turbulent mixing of a passive and chemically reacting species in a low-speed shear layer. *J. Fluid Mech.* **82**, 53–95.

BECHERT, D. & PFIZENMAIER, E. R. 1975 On wavelike perturbations in a free jet travelling faster than the mean flow in the jet. *J. Fluid Mech.* **72**, 341–352.

BLACKWELDER, R. 1977 On the role of phase information in conditioned sampling. *Phys. Fluids* **20**, 5232–5242.

BRADSHAW, P., FERRISS, D. H. & ATWELL, N. P. 1967 Calculation of boundary-layer development using the turbulent energy equation. *J. Fluid Mech.* **28**, 593–616.

BRUNN, H. H. 1977 A time-domain analysis of the large-scale flow structure in a circular jet. Part 1. Moderate Reynolds number. *J. Fluid Mech.* **83**, 641–671.

BULL, M. K. 1967 Wall pressure fluctuations associated with subsonic turbulent boundary flow. *J. Fluid Mech.* **28**, 719–754.

BULLOCK, K. J., COOPER, R. E. & ABERNATHY, F. H. 1978 Structural similarity in radial correlations and spectra of longitudinal velocity fluctuations in pipe flow. *J. Fluid Mech.* **88**, 585–608.

CHAMPAGNE, F. H., HARRIS, V. G. & CORRSIN, S. 1970 Experiments on nearly homogeneous turbulent shear flow. *J. Fluid Mech.* **41**, 81–139.

CHANAUD, R. C. & HAYDEN, R. E. 1970 Edge noise caused by two turbulent wall jets. *J. Acoust. Soc. Am.* **48**, 125.

COMTE-BELLOT, G. & CORRSIN, S. 1971 Single Eulerian time correlation of full and narrow-band velocity signals in grid-generated 'isotropic' turbulence. *J. Fluid Mech.* **48**, 273–337.

CROCOS, G. M. 1962 Pressure fluctuations in shear flows. *Univ. California, Inst. Engng Res. Rep. Ser.* 183, no. 2.

DAVIES, P. O. A. L., FISHER, M. J. & BARRATT, M. J. 1963 The characteristic of the turbulence in the mixing region of a round jet. *J. Fluid Mech.* **15**, 337–367.

DAVIS, M. R. 1975 Intensity, scale and convection of turbulent density fluctuations. *J. Fluid Mech.* **70**, 463–479.

DEMETRIADES, A. 1976 Turbulence correlations in a compressible wake. *J. Fluid Mech.* **74**, 251–267.

DINKELACKER, A., HESSEL, M., MEIER, G. E. A. & SCHEWE, G. 1977 Investigation of pressure fluctuations beneath a turbulent boundary layer by means of an optical method. *Phys. Fluids* **20**, 5216–5224.

FAVRE, A. J., GAVIGLIO, J. & DUMAS, R. 1967 Structure of velocity space–time correlations in a boundary. *Phys. Fluids Suppl.* **10**, 5138–5145.

FAVRE, A. J. 1965 Review of space–time correlations in turbulent fluids. *Trans. A.S.M.E.* E, *J. Appl. Mech.* **32**, 241–257.

FISHER, J. J. & DAVIES, P. O. A. L. 1964 Correlation measurements in a non-frozen pattern of turbulence. *J. Fluid Mech.* **18**, 99–116.

FRENKIEL, F. N. & KLEBANOFF, P. 1966 Space–time correlations in turbulence. *Dynamics of Fluids and Plasmas* (ed. S. I. Pai), pp. 257–274. Academic.

GOLDSCHMIDT, V. W. & YOUNG, M. F. 1975 Energy spectrum and turbulent scales in a plane air jet. *Proc. 4th Biennial Symp. on Turbulence in Liquids* (ed. J. L. Zakin & G. K. Patterson), pp. 39–45. N.Y.: Science.

GUTMARK, E. & WYGNANSKI, I. 1976 The planar turbulent jet. *J. Fluid Mech.* **73**, 465–495.

HUSSAIN, A. K. M. F. & ZAMAN, K. B. M. 1978 The free shear layer tone phenomenon and probe interference. *J. Fluid Mech.* **87**, 349–383.

HEIDRICK, T., AZAD, R. S. & BANERJEE, S. 1971 Phase velocities and angle of inclination for frequency-components in fully developed turbulent flow through pipes. *Symp. on Turbulence in Liquids, Univ. Missouri-Rolla.*

HEIDRICK, T. R., BANERJEE, S. & AZAD, R. S. 1977 Experiments on the structure of turbulence on fully developed pipe flow: interpretation of the measurements by a wave model. *J. Fluid Mech.* **81**, 137–154.

HESKESTAD, G. 1965 A generalized Taylor hypothesis with application for higher Reynolds number turbulent shear flow. *Trans. A.S.M.E.* E, *J. Appl. Mech.* **32**, 735–739.

JENKINS, P. E. & GOLDSCHMIDT, V. W. 1976 Conditional (point averaged) temperature and velocities on a heated turbulent plane jet. *Phys. Fluids* **19**, 613–617.

JONES, B. G., PLANCHON, H. P. & HAMMERSLEY, R. J. 1973 Turbulent correlation measurements in a two-stream mixing layer. *A.I.A.A. J.* **11**, 1146–1150.

KO, N. W. M. & DAVIES, P. O. A. L. 1971 The near field within the potential core of subsonic cold jets. *J. Fluid Mech.* **50**, 49–78.

KOVASZNAY, L. S. G., KIBENS, V. & BLACKWELDER, R. F. 1970 Large-scale motion in the intermittent region of a turbulent boundary layer. *J. Fluid Mech.* **41**, 283–325.

LAU, J. C. & FISHER, M. J. 1975 The vortex-street structure of turbulent jets. Part 1. *J. Fluid Mech.* **67**, 299–337.

LIN, C. C. 1953 On Taylor's hypothesis and the acceleration terms in the Navier–Stokes equation. *Quart. Appl. Math.* **10**, 295–306.

LUMLEY, J. L. 1965 Interpretation of time spectra measured in high-intensity shear flows. *Phys. Fluids* **8**, 1056–1062.

MCCONACHIE, P. J., BULLOCK, K. J. & KRONAUER, R. E. 1977 Distribution of convection velocities in turbulent pipe flow. *Univ. Queensland, Res. Rep.* no. 2/77. (See also K. J. Bullock *et al.* 1978.)

MIKSAD, R. W. 1972 Experiments on the nonlinear stages of free-shear layer transition. *J. Fluid Mech.* **56**, 695–719.

OSWALD, L. & KIBENS, V. 1971 Turbulent flow in the wake of a disk. *Univ. Michigan, College Engng, Tech. Rep.* 002820, pp. 1–15.

OTT, E. S. 1972 Convective velocities in a turbulent plane jet. Master's thesis, Purdue University.

RAJAGOPOLAN, S. & ANTONIA, R. A. 1980 Interaction between large and small scale motions in a two-dimensional turbulent duct flow. *Phys. Fluids* **23**, 1101–1110.

ROBINS, A. G. 1973 Ph.D. thesis, London University.

ROTTA, J. C. 1962 Turbulent boundary layers in incompressible flow. *Progress in Aeronautical Sciences, Vol. 2. Boundary Layer Problems*, pp. 1–221. Pergamon.

SCHLICHTING, W. 1955 *Boundary Layer Theory*. McGraw-Hill.

SEPRI, P. 1976 Two-point turbulence measurements downstream of a heated grid. *Phys. Fluids* **19**, 1876–1884.

STERNBERG, J. 1967 On the interpretation of space–time correlation measurements in shear flow. *Phys. Fluids Suppl.* **10**, 5146–5152.

TAYLOR, G. I. 1935 Statistical theory of turbulence. Part 1. *Proc. Roy. Soc.* A **151**, 421–444.

WILLMARTH, W. W. 1959 Space–time correlations and spectra of wall pressure in a turbulent boundary layer. *N.A.S.A. Memo* 3-17-59 W.

WILLMARTH, W. W. & WOOLDRIDGE, C. E. 1962 Measurements of the fluctuating pressure at the wall beneath a thick turbulent boundary layer. *J. Fluid Mech.* **11**, 187–210.

WILLS, J. A. B. 1964 On convection velocities in turbulent shear flows. *J. Fluid Mech.* **20**, 417–432.

WILSON, L. W. & DAMKEVALA, R. J. 1970 Statistical properties of turbulent density fluctuations. *J. Fluid Mech.* **42**, 291–303.

WOOLDRIDGE, L. E., WOOTEN, D. C. & AMARO, A. J. 1972 The structure of jet turbulence producing jet noise. *A.I.A.A. J.* **10**, 72–158.

WOOTEN, D. C., WOOLDRIDGE, C. E., AMARO, A. J. & PLAPP, G. R. 1971 A study of the structure of jet turbulence producing jet noise. *N.A.S.A.* CR-1836.

WYGNANSKI, I. & FIEDLER, H. 1969 Some measurements in the self-preserving jet. *J. Fluid Mech.* **38**, 327–361.

WYGNANSKI, I. & FIEDLER, H. 1970 The two dimensional mixing region. *J. Fluid Mech.* **41**, 327–361.